Effect of solution treatment conditions on the sensitization of austenitic stainless steel

XIAOFEI YU[1], SHENHAO CHEN[1,2]* and LIANG WANG[1]

[1]*Department of Chemistry, Shandong University, Jinan 250100 and* [2]*State Key Laboratory for Corrosion and Protection, Shenyang 110016, PR China*

Abstract: In this study, the impact of the conditions of solution treatment on the degree of sensitization (DOS) of austenitic stainless steel (AISI 304) was investigated in detail. The results derived from the electrochemical potentiodynamic reactivation (EPR) test indicated that the DOS decreased as the solution treatment temperature and time increased. The reason for this was studied *via* the SEM morphologies and EDS results, which indicated that the grain size influenced the DOS. Furthermore, cellular automaton (CA) was utilized to simulate grain growth, the precipitation of Cr-rich carbides and the three dimensional distribution of the chromium concentration, which vividly illuminated the effect of the grain size on the DOS and was in accordance with the experiment results.

Keywords: intergranular corrosion; degree of sensitization; cellular automaton; austenitic stainless steel.

INTRODUCTION

Stainless steels have excellent corrosion resistance when properly heated and used in a low temperature environment. However, they are vulnerable to corrosion when exposed to temperatures between 450 and 900 °C.[1–4] This is because the formation of Cr-rich carbides at the grain boundaries extracts chromium from the grain boundaries and neighboring matrix, leaving a Cr-depleted zone extending to both sides of the grain boundaries. The Cr-depleted zone is vulnerable to attack, leading to intergranular corrosion (IGC) or stress cracking corrosion.[5–8] In order to correlate IGC with the grain boundary characteristics, many studies have been devoted to the quantitative evaluation of the depleted zones by empirical or analytical models.[9–15]

Generally, these models are successful in calculating the chromium concentration profiles and their evolutions during aging. However, the chromium con-

---

* Corresponding author. E-mail: shchen@sdu.edu.cn

Available online at www.shd.org.rs/JSCS/

centration profiles can only reflect the distribution along a certain direction, rather than giving an overall view of the chromium distribution. Therefore, the intention of this work was to simulate the chromium distribution in a three dimensional manner. As an important algorithm, CA, that describes the discrete spatial and temporal microstructure evolution on a mesoscale, was applied to simulate recrystallization, grain coarsening, phase transformation and grain growth.[16–25] However, hitherto, there has been no report about the employment of the CA to investigate IGC of austenitic stainless steel, except the simulation of general corrosion of a metal with defects.[26] Based on the above-mentioned, the CA was adopted to study the effect of solution treatment conditions on the degree of sensitization (DOS) of austenitic stainless steel (AISI 304), and the evolution of grain growth, the precipitation of Cr-rich carbides and the distribution of the chromium concentration are presented herein.

EXPERIMENTAL

Experiments

The steel (AISI 304) with a diameter of 3 mm investigated in this study contained of 0.055 % C, 1.00 % Mn, 8.48 % Ni, 0.600 % Si, 0.029 % P, 0.005 % S, 18.28 % Cr and Fe in balance. The samples were first solution treated at 900, 1000 and 1100 °C for 0, 15, 30 min, 1 h and 2 h and then sensitized at 650 °C for 12 h. After the pretreatment, the specimens were sealed with epoxy resin, with only the working area exposed. The electrodes were polished with emery paper to mirror-like brightness, rinsed with alcohol and Milli-Q ultrapure water before the electrochemical experiments.

The DOS of the samples was determined by the electrochemical potentiodynamic reactivation (EPR) test.[2] All the experiments were repeated several times and the average values represented the DOS. After the electrochemical experiments, the electrodes were cleaned in Milli-Q ultrapure water, immersed in alcohol and cleaned in an ultrasonic cleaner for 15 min, dried in air, and then EDS and SEM measurements were performed using a JSM-6700F filed emission scanning electron microscope (Japan JEOL).

CA simulation model

The initial microstructure, used to simulate the precipitation of Cr-rich carbides and the distribution of the chromium concentration, resulted from grain growth at different temperatures. The detailed theory about grain growth can be found in the literature.[19-25]

For the simulation of the precipitation of Cr-rich carbides, a nucleation model based on the classical nucleation theory was employed. This model can be described as follows:[20-22]

$$I = K_1 D_\gamma (kT) \exp(-K_2/kT(\Delta G)^2), \tag{1}$$

where I is the nucleation density, K_1 is a constant related to the nucleation site density, K_2 is a constant related to all the interfaces involved in the nucleation, D_γ is the chromium diffusion coefficient, k is the Boltzmann constant and ΔG is the driving force.

Moreover, the growth of the carbides was assumed to be controlled by both the chromium diffusion and the interface mobility. As the interface moves during the precipitation, chromium atoms transfer from the matrix to the interface and then they precipitate to the carbides. Consequently, the growth of carbides can be described as a free boundary problem

Available online at www.shd.org.rs/JSCS/

for chromium diffusion in austenite and the dynamics of the interface. The chromium diffusion in austenite is described as follows:

$$dc/dt = \nabla(D\nabla c), \tag{2}$$

where c is the chromium concentration and D is the chromium diffusion coefficient.

Allowing for the characteristics of the precipitation of Cr-rich carbides, the mobility of interface is equal to the growth of carbides and the length that the interface covers can be expressed by:[14,15]

$$l = \beta\sqrt{Dt}, \tag{3}$$

where t is the sensitization time, β is a constant and D is the chromium diffusion coefficient, which, being a thermally activated process, depends on the temperature. All of the key parameters are listed in Table I.

TABLE I. The key parameters used in the present model

M_0 / m^4 J^{-1} s^{-1}	γ_m / J m^{-2}	θ_m / °	a / μm	β	Q / kJ mol^{-1} (taken from[14,18])
1.56×10^{-11}	0.56	15 deg	1	0.137	245.7

RESULTS AND DISCUSSION

The effect of solution treatment temperature on the sensitization

The influence of the solution treatment temperature on the susceptibility to IGC was studied at 900, 1000 and 1100 °C while the other conditions were maintained constant. The DOS obtained from the EPR test is shown in Fig. 1, from which it can be seen that the DOS decreased gradually with increasing temperature irrespective of the treatment time. For example, when the samples were
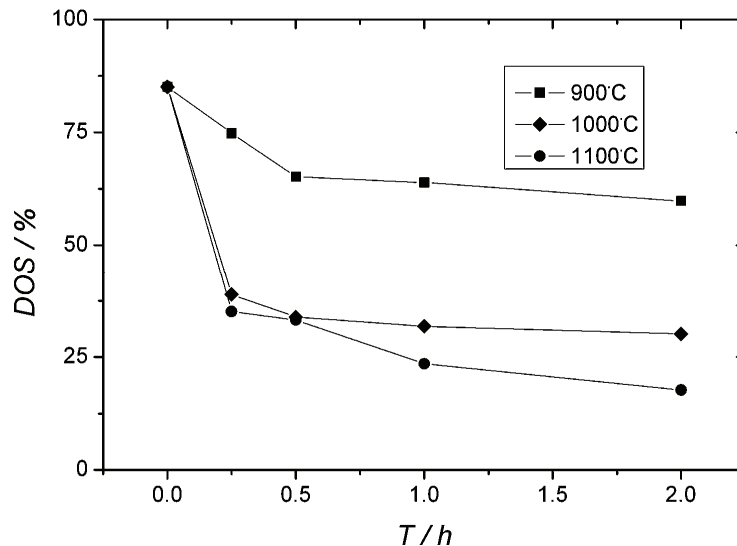

Fig. 1. The DOS obtained from the EPR test.

treated at 900, 1000 and 1100 °C for 1 h and then sensitized at 650 °C for 12 h, the DOS was 63.9, 31.8 and 23.5 % respectively. The changing trend of the DOS were the same when the solution treatment time was 15 min, 30 min and 2 h. The SEM morphologies shown in Fig. 2 were taken after the EPR test and revealed that IGC occurred at all three temperatures. However, the degree of IGC was reduced as the temperature increased.
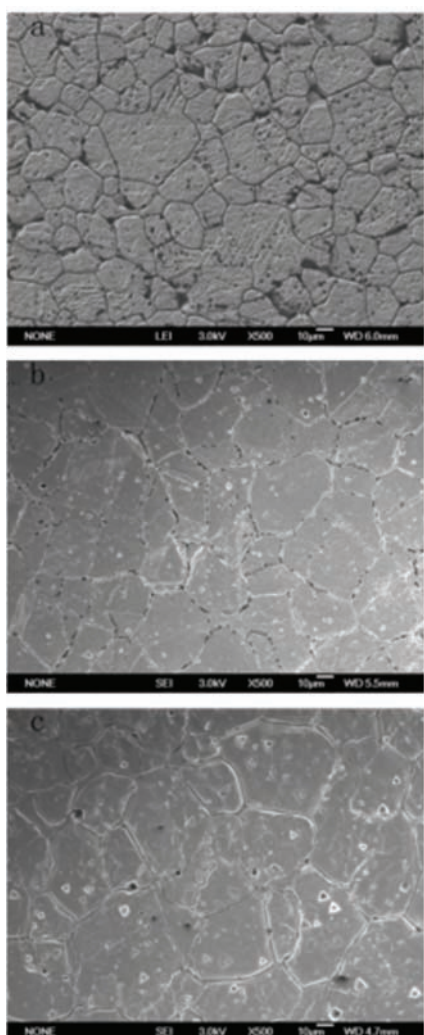

Fig. 2. SEM Morphologies of the samples heated at: a) 900, b) 1000 and c) 1100 °C for 0.5 h, and then sensitized at 650 °C for 12 h.

The effect of solution treatment time on the sensitization

Figure 1 not only shows the effect of solution treatment temperature on the DOS, but also indicates the impact of the treatment time on it. From the Figure, it

can be seen that the DOS for the sample without heat treatment was very high, but it decreased sharply for the samples subjected to heat treatment. When the samples were heated at 1100 °C for 15 min to 2 h, the DOS decreased from 35.1 to 17.7 %. At the other temperatures, the DOS also decreased as the time increased. The SEM morphologies of the samples heated at 1100 °C for 15 min, 30 min and 2 h and then sensitized at 650 °C for 12 h after the EPR test are shown in Fig. 3. The figure reveals that IGC occurred under all conditions, but it was reduced as the time was prolonged.
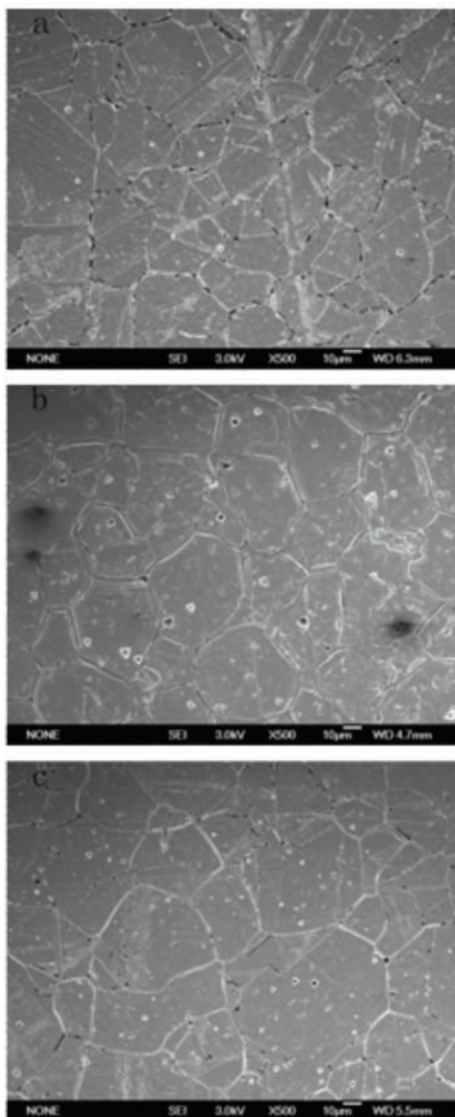

Fig. 3. SEM Morphologies of the samples heated at 1100 °C for: a) 15 min, b) 30 min and c) 2 h, and then sensitized at 650 °C for 12 h.

The effect of grain size on the sensitization

Grain size is one of the most important factors that can affect IGC and it mainly affects the time required to reach the state of complete sensitization.[27,28] The relationship between the grain size and the time to attain the state of complete sensitization can be expressed as:

$$t_{max,1} = (d_1/d_2)^{2/3} t_{max,2} \qquad (4)$$

where $t_{max,1}$ and $t_{max,2}$ are the times required to reach the state of complete sensitization, and d_1 and d_2 are the grain sizes.[12] The chromium concentration at the grain boundaries at any sensitization time during the sensitization stage is related to t_{max} and is defined as:

$$c = c_0 \exp(-kt/t_{max}), \qquad (5)$$

where c is the chromium concentration at the grain boundaries at sensitization time t, c_0 is the initial concentration of chromium, t is the sensitization time, t_{max} is the time required to reach the state of complete sensitization and k is a constant.[15]

From these two equations, it can be assumed that if t is shorter than t_{max} and is kept the same for the different grain size samples, the chromium concentration at the grain boundaries of a large grain sample will be higher than that of a small grain one. This means the precipitation of a large grain sample will be less than that of a small grain one. As a result, the DOS of a large grain sample will be lower than that of a small grain one, which is determined by the volume of precipitation.

Although the grain boundary surface area became smaller as the grains grew larger, the precipitation of Cr-rich carbides per grain boundary surface area increased. The reason is that the samples were derived from the same material and the sensitization was performed at the same temperature. Hence, the precipitation volume was the same for the different grain size samples. However, as the grain size becomes larger, the chromium atoms must diffuse a longer distance to reach the grain boundaries and this is a time consuming procedure. Hence, if the sensitization time is very short, the DOS of the larger grain samples may be lower than that of the smaller grain samples. Through experiments, it was found that the DOS of the smallest grain sample was still increasing when the sensitization time was 192 h. Thus, the sensitization time of 12 h used in this study was shorter than the smallest t_{max}. As a result, the DOS of the large grain sample was lower than that of the small grain sample.

From the SEM morphologies exhibited in Figs. 2 and 3, it can be observed that the grain size became larger as the temperature and time increased. The average grain sizes obtained from Fig. 2 were 19.5, 22.8 and 26.8 μm, respectively, while those obtained from Fig. 3 were 20.8, 23.6 and 37.8 μm, respectively. In

Available online at www.shd.org.rs/JSCS/

order to prove if it was the grain size that influenced the DOS, the chromium concentration at grain boundaries was determined by EDS. The measurement of the chromium concentration at the grain boundaries of each sample was repeated five times and the final concentration was the average value of the five determined values. According to Eqs. (1) and (2), $d^{2/3}$ should change linearly with $1/\ln(c)$. The relationship between the grain size and the chromium concentration is presented in Fig. 4. Allowing for experiment error, the results were in agreement with the theoretical calculation. This suggests that it was the grain size that had an impact on the DOS.
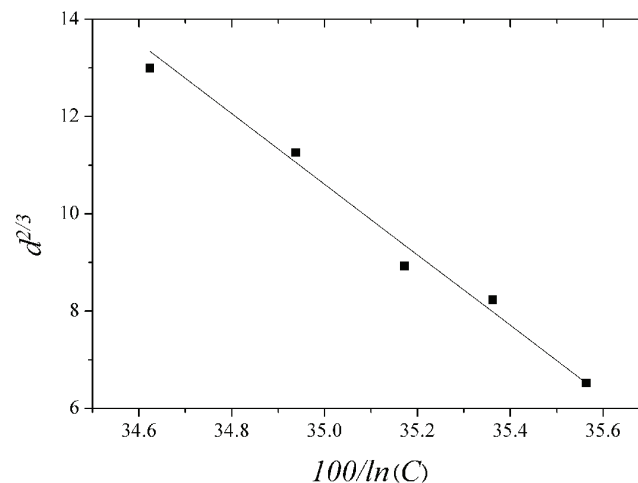

Fig. 4. The relationship between the grain size and the chromium concentration.

In order to show the effect of grain size on the DOS, the CA was utilized to simulate the precipitation of Cr-rich carbides and the distribution of the chromium concentration. The simulation was performed on a 100×100 square lattice and the distance between two neighboring cells was 1.0 µm. The state of each lattice site was characterized by four state variables: the grain orientation variable representing the different grains; the phase state variable indicating whether it belonged to the carbides, the matrix, or the carbides/matrix interface; the fraction variable representing the fraction of carbides in an interface cell, and the chromium concentration. The Moore neighbor rule, which considers the first and the second nearest eight neighbors, was employed. The procedure and the transition rules were as follows: first, the initial variables for each cell were assigned, and then nucleation occurred randomly to those cells belonging to the preferential nucleation sites according to the nucleation model. In addition to nucleation, the carbides formed at the other steps would simultaneously grow into the matrix. When the fraction of the carbides in an interface cell was no less than one unit,

the phase state variable of this cell would change into the phase state variable of the carbides and the orientation variable was given randomly. At the same time, all its neighboring austenite cells changed their phase state variables into the phase state variable of the interface. In addition, the chromium concentration at each site was calculated according to Eq. (2). Lastly, the variables for each cell were updated and the simulation cycle was repeated until the simulation was completed.

The microstructures used to study the effect of grain size on the precipitation of Cr-rich carbides, which were obtained from grain growth at 900, 1000 and 1100 °C, are displayed in Fig. 5. The average grain sizes were 19.7, 22.5 and 26.5 μm, respectively, and were almost equal to the grain sizes of the material. The changes of the precipitation together with the grain size are shown in Fig. 6, from which it can be clearly seen that the volume of precipitate decreased with increasing grain size. The corresponding distribution of the chromium concentration, which clearly reflects the changes in the precipitation, is presented in Fig. 7. The concentration at the grain boundaries for the large grain sample was higher than that for the small grain one, which is in accordance with the experiment results. Hence, the simulation clearly showed the effect of the solution treatments on the DOS.
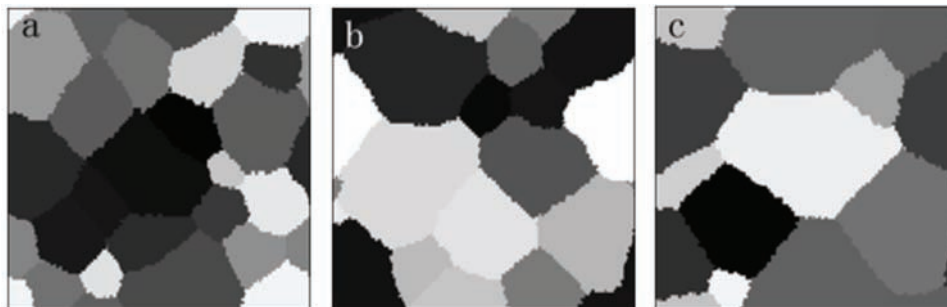

Fig. 5. The microstructure obtained from grain growth at different temperatures: a) 900, b) 1000 and c) 1100 °C.
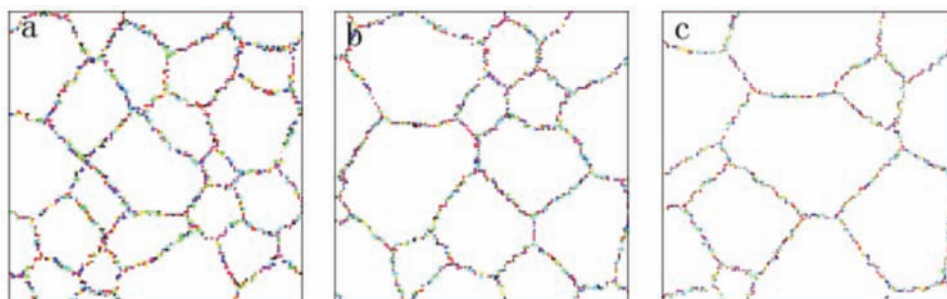

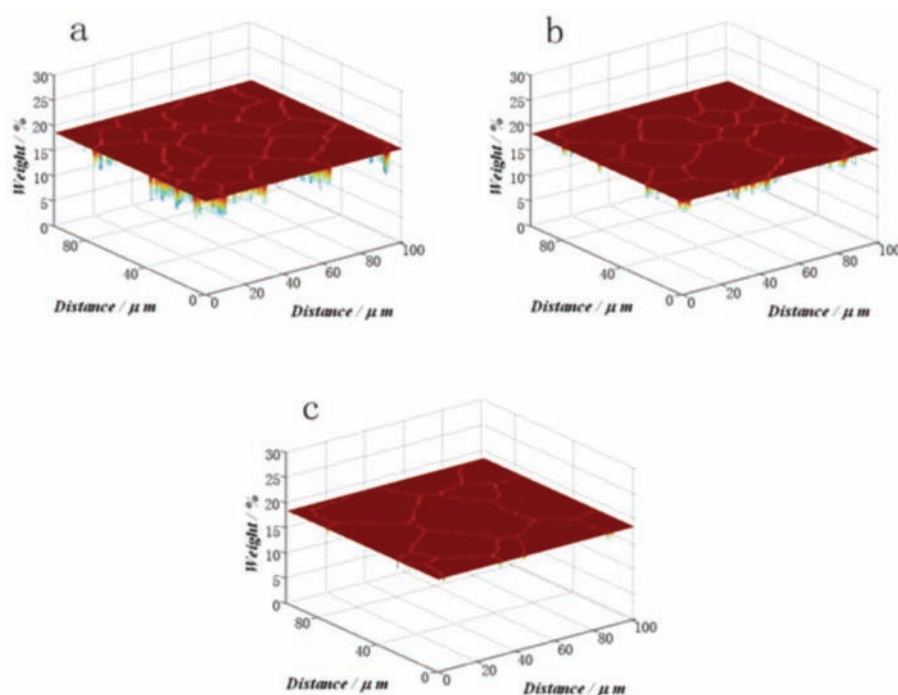Fig. 6. Effect of grain size on the precipitation: a) 19.7, b) 22.5 and c) 26.5 μm.

Fig. 7. The distribution of the chromium concentration corresponding to Fig. 6.

CONCLUSIONS

The effect of solution treatment conditions on the DOS of AISI 304 austenitic stainless steel was studied experimentally and by simulation methods. The experimental results showed that the DOS decreased as the temperature and time of the solution treatment increased. In order to understand the relationship between the DOS and the solution treatment temperature and time, a CA was used to simulate the grain growth, the precipitation and the three dimensional distribution of the chromium concentration, which perfectly explained the influence of temperature and time on the DOS.

И З В О Д

УТИЦАЈ УСЛОВА ТРЕТМАНА У РАСТВОРУ НА ПОВЕЋАЊЕ ОСЕТЉИВОСТИ АУСТЕНИТНОГ ЧЕЛИКА

XIAOFEI YU[1], SHENHAO CHEN[1,2] и LIANG WANG[1]

[1]*Department of Chemistry, Shandong University, Jinan 250100 u* [2]*State Key Laboratory for Corrosion and Protection, Shenyang 110016, PR China*

У раду је детаљно испитан утицај услова третмана у раствору на степен повећања осетљивости аустенитног челика (AISI 304). Резултати теста електрохемијске потенциостатске

реактивације указују да степен повећања осетљивости опада са повећањем температуре и времена третмана у раствору. Узроци таквог понашања су тражени у морфологији (која је одређена скенирајућом електронском микроскопијом, SEM) и резултатима енергетско-дисперзионе анализе X-зрацима (EDS). Показало се да величина зрна утиче на степен повећања осетљивости. Поред тога, моделом ћелијских аутомата су симулирани раст зрна, таложење карбида богатих хромом и тродимензиона расподела концентрације хрома, што је сликовито објаснило ефекат величине зрна на степен повећање осетљивости аустенитног челика који је експерименално утврђен.

REFERENCES

1. R. Singh, J. Mater. *Proc. Techol.* **206** (2008) 286
2. R. Singh, B. Ravikumar, A. Kumar, P. K. Dey, I. Chattoraj, *Metall. Mater. Trans. A* **34** (2003) 2441
3. G. Radenković, S. K. Zečević, Z. Cvijović, D. M. Dražić, *J. Serb. Chem. Soc.* **60** (1995) 53
4. H. Ma, S. Chen, C. Yang, J. Luo, *J. Serb. Chem. Soc.* **67** (2002) 425
5. Y. F. Cheng, L. Niu, *Electrochem. Commun.* **9** (2007) 558
6. R. Nishimura, A. Sulaiman, Y. Maeda, *Corros. Sci.* **45** (2003) 465
7. R. Nishimura, Y. Maeda, *Corros. Sci.* **45** (2003) 1847
8. G. H. Aydoğdu, M. K. Aydinol, *Corros. Sci.* **48** (2006) 3565
9. J. J. Kai, G. P. Yu, C. H. Tsai, M. N. Liu, S. C. Yao, *Metall. Trans. A* **20** (1989) 2057
10. C. Strawstrom, M. Hillert, *J. Iron Steel Inst.* **207** (1969) 77
11. G. S. Was, R. M. Kruger, *Acta Metall.* **33** (1985) 841
12. Y. F. Yin, R. G. Faulkner, *Corros. Sci.* **49** (2007) 2177
13. H. Sahlaoui, K. Makhlouf, H. Sidhom, J. Philibert, *Mater. Sci. Eng. A* **372** (2004) 98
14. W. E. Mayo, *Mater. Sci. Eng. A* **232** (1997) 129
15. H. Sahlaoui, H. Sidhom, J. Philibert, *Acta Mater.* **50** (2002) 1383
16. R. Ding, Z. X. Guo, *Acta Mater.* **49** (2001) 3163
17. G. Kugler, R. Turk, *Acta Mater.* **52** (2004) 4659
18. Y. J. Lan, D. Z. Li, Y. Y. Li, *Metall. Mater. Trans. B* **37** (2006) 119
19. J. Geiger, A. Roósz, P. Barkóczy, *Acta Mater.* **49** (2001) 623
20. Y. J. Lan, D. Z. Li, Y. Y. Li, *Acta Mater.* **52** (2004) 1721
21. S. Kundu, M. Dutta, S. Ganguly, S. Chandra, *Scripta Mater.* **50** (2004)891
22. Y. J. Lan, N. M. Xiao, D. Z. Li, Y. Y. Li, *Acta Mater.* **53** (2005) 991
23. S. Raghavan, S. S. Sahay, *Mater. Sci. Eng. A* **445**–**446** (2007) 203
24. Y. Z. He, H. L. Ding, L. F. Liu, K. Shin, *Mater. Sci. Eng. A* **429** (2006) 236
25. H. L. Ding, Y. Z. He, L. F. Liu, W. J. Ding, *J. Cryst. Growth* **293** (2006) 489
26. A. Taleb, J. Stafiej, J. P. Badiali, *J. Phys. Chem. C* **111** (2007) 9086
27. R. Singh, S. G. Chowdhury, B. Ravikumar, S. K. Das, P. K. Dey, I. Chattoraj, *Scripta Mater.* **57** (2007) 185
28. R. Beltran, J. G. Maldonado, L. E. Murr, W. W. Fisher, *Acta Mater.* **45** (1997) 4351.